Journal of Alloys and Compounds 509 (2011) L85–L89

Contents lists available at ScienceDirect

Journal of Alloys and Compounds

journal homepage: www.elsevier.com/locate/jallcom

Letter

Ru incorporation on marked enhancement of diffusion resistance of multi-component alloy barrier layers

Shou-Yi Chang*, Chen-Yuan Wang, Ming-Ku Chen, Chen-En Li

Department of Materials Science and Engineering, National Chung Hsing University, Taichung 40227, Taiwan

ARTICLE INFO

Article history:
Received 24 June 2010
Received in revised form
11 November 2010
Accepted 19 November 2010
Available online 26 November 2010

Keywords:
Interconnect
Diffusion barrier
High-entropy alloy

ABSTRACT

In this study, amorphous AlCrTaTiZr quinary alloy and 20 at.% Ru-incorporated AlCrTaTiZrRu senary alloy films were developed as diffusion barrier layers to inhibit Cu diffusion in interconnect structures. Under annealing at 700 °C, the interdiffusion of Cu and Si through the AlCrTaTiZr quinary alloy layer of 50 nm thick occurred, and compounds including Cu_3Si consequently formed. In comparison, at 800 °C, the interdiffusion was still effectively retarded by the Ru-incorporated AlCrTaTiZrRu senary alloy layer of only 5 nm thick without obvious formation of silicides. It suggests the high diffusion resistance of the Ru-incorporated barrier layer possibly attributed to the large lattice distortions caused by the addition of extra-large-sized Ru atoms.

1. Introduction

The nitride films of transition metals, such as TiN and TaN, have been widely used as barrier layers in interconnects to inhibit rapid Cu diffusion [1–5]. However, microstructure defects, such as grain and column boundaries, formed in these conventional barrier layers provide some paths for rapid Cu diffusion and consequently lower the diffusion resistance of the barrier layers. To fulfill the strict demands for Cu interconnects in the manufacturing generations below 65 nm, other barrier systems with ternary components or composition modifications [6–11], e.g., Ru–Ti–N and Ru–Ta–N [10,11], and/or of layered structures [12–18], including Ta/TaN and Ru/TaN [16–18], to elongate diffusion distances have received considerable interest and are continually developed. However, proper barrier layers for 32 or 22 nm generation with a low electrical resistivity, an ultra-small thickness around 5 nm, and still a high diffusion resistance have seldom been reported.

In 2004, Yeh developed the high-entropy alloys (denoted as HEAs) with the addition of multiprincipal (more than five) elements [19–22]. The high mixing entropies contributed by multiprincipal components stabilize simple solid-solution structures [19]. In addition, large lattice distortions caused by different atomic sizes lower the diffusion rates of atoms; therefore, many of the HEAs possess nanocrystalline or even amorphous structures, and exhibit excellent properties [19–22]. Thin films of the HEAs and HEA nitrides (denoted as HEANs) can also be deposited by a simple sputtering process [19,23–26]. In particular, the HEANs have received considerable interest as diffusion barrier layers for Cu interconnects owing to the anticipated high diffusion resistance provided by their amorphous structures and also large lattice distortions [24–26].

However, the high electrical resistivity (>1500 μΩ cm) of the previously developed HEAN (nitride) films renders their applications infeasible. Alternatively, a metallic alloy film with a low electrical resistivity and still a high diffusion resistance is demanded. Thus, in this work, an AlCrTaTiZr quinary high-entropy alloy (QHEA) film is further developed. To utilize the effect of large lattice distortions on the enhancement of diffusion resistance, 20 at.% Ru with an extra-large atomic size of 3.56 Å is incorporated in the quinary alloy to form an AlCrTaTiZrRu senary high-entropy alloy (SHEA) film. The interdiffusion of Cu and Si through the QHEA and SHEA barrier layers at high temperatures is characterized to examine their diffusion resistance.

2. Experimental

The QHEA and SHEA films were deposited on Si substrates by a radio-frequency (rf) magnetron sputtering process. The sputtering targets were prepared with equimolar Al, Cr, Ta, Ti, Zr and Al, Cr, Ta, Ti, Zr, Ru, respectively, by vacuum arc-melting the constituent elements, followed by cutting and polishing of the solidified bulks into discs of 50 mm in diameter. The QHEA film of about 50 nm thick and the SHEA film of about 5 nm thick were deposited at an rf power of 150 W and a substrate bias of −100 V in an Ar atmosphere (working pressure of 6×10^{-3} Torr) at room temperature. On the QHEA and SHEA layers, a Cu film of about 400–450 nm thick was subsequently deposited under a power of 50 W to obtain Si/QHEA/Cu and Si/SHEA/Cu film stacks. To examine the interdiffusion behaviors of Cu and Si through

* Corresponding author at: Department of Materials Science and Engineering, National Chung Hsing University, 250 Kuo Kuang Rd., Taichung 40227, Taiwan. Tel.: +886 4 22857517; fax: +886 4 22857017.
E-mail address: shouyi@dragon.nchu.edu.tw (S.-Y. Chang).

0925-8388/$ – see front matter © 2010 Elsevier B.V. All rights reserved.
doi:10.1016/j.jallcom.2010.11.124

Table 1
Chemical compositions of as-deposited QHEA and SHEA film determined by EPMA as well as the crystal structures and atomic sizes of incorporated metallic elements.

Element	Al	Cr	Ta	Ti	Zr	Ru
Content (QHEA, at.%)	8.10	24.52	22.55	20.45	20.53	–
Content (SHEA, at.%)	10.28	18.75	17.58	14.85	15.08	19.52
Crystal structure	fcc	bcc	bcc	hcp	hcp	hcp
Atomic size (Å)	2.864	2.498	2.856	2.896	3.179	3.560

fcc: face-centered cubic; bcc: body-centered cubic; hcp: hexagonal close-packed.

the QHEA and SHEA barrier layers, thermal annealing was applied to the film stacks at 600–900 °C for 30 min in a vacuum of 2×10^{-5} Torr.

The chemical compositions of as-deposited QHEA and SHEA films (~500 nm thick) were determined by field-emission electron probe micro-analyses (EPMA, JEOL JXA-8800M). The morphologies of Si/QHEA/Cu and Si/SHEA/Cu film stacks were observed by a scanning electron microscope (SEM, JEOL JSM-6700F). The crystal structures were analyzed using a glancing incident angle (0.5°) X-ray diffractometer (XRD, Rigaku Dmax 2000). The microstructures and lattice images of as-deposited and thermally annealed film stacks were examined by a high-resolution transmission electron microscope (HRTEM, JEOL JEM-3000F). The sheet resistance of the QHEA and SHEA films (~500 nm thick) as well as the film stacks was measured by a four-point probe station (Keithley 2400).

3. Results and discussion

Table 1 first lists the chemical compositions of as-deposited QHEA and SHEA films determined by EPMA, as well as the crystal structures and atomic sizes of the incorporated metallic elements. It was clear that, except the lower Al contents than the designed values due to a resputtering effect of the light element, the contents of the other metallic elements in the QHEA and SHEA films were approximately 20–25 and 15–20 at.%, respectively, in near-equimolar ratios and close to the designed compositions. The electrical resistivities of the deposited QHEA and SHEA films were measured as 250 and 246 μΩ cm, respectively, which were lower than the values of TaN and other typical nitride-based barrier materials, and suggested the potential of the QHEA and SHEA films for diffusion barrier applications [4]. Moreover, Fig. 1 shows the HRTEM images of the as-deposited Si/QHEA/Cu and Si/SHEA/Cu film stacks; the layer-stacked structures of the Si substrate, native oxide layer, barrier layer and Cu film were clearly observed (the Cu film and a part of the QHEA layer in Fig. 1(a) were lost during sample preparation). Under detailed lattice examinations, as seen in the magnified images around the barrier layers inserted in the up-right corners, both the QHEA and the SHEA layers were identified as an amorphous structure. Within them, large lattice distortions were expected to exist due to the marked differences in the atomic sizes of the incorporated elements as listed in Table 1, particularly in the SHEA layer with the addition of 20 at.% Ru with an extra-large atomic size of 3.56 Å. Not any intermetallic compounds or crystalline phases were found in the amorphous QHEA and SHEA layers, implying the random solid solution of all the incorporated metallic elements attributed to the effect of high mixing entropies [19].

Fig. 2 shows the XRD patterns of the Si/QHEA/Cu and Si/SHEA/Cu film stacks before and after annealing at 600–900 °C. The diffraction peaks at 43.4°, 50.6° and 74.3° corresponded to the (1 1 1), (2 0 0) and (2 2 0) lattice planes of face-centered cubic Cu. Just at 700 °C, the QHEA layer of 50 nm thick failed as an effective diffusion barrier. Two peaks around 44.7–45.4° appeared in the XRD pattern of the 700 °C-annealed Si/QHEA/Cu film stack, indicating the interdiffusion of Cu and Si through the QHEA barrier layer, and the subsequent formation of Cu_3Si compound phase. Some other compound or solution phases formed as well due to the reactions between the QHEA layer and the Si substrate or Cu film, such as Ta–Si based ($TaSi_2$, Ta_5Si_3) and Al–Cu–Zr based ($AlCu_2Zr$, Al_3Zr_4) ones. In comparison with the typical morphology of as-deposited

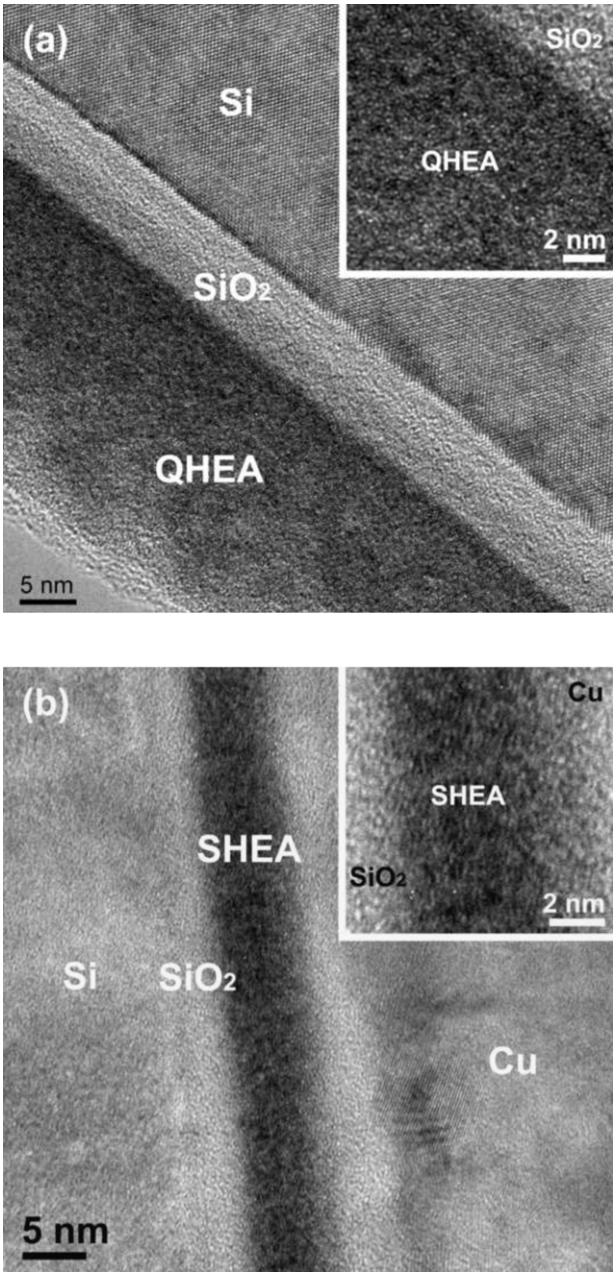

Fig. 1. HRTEM images of as-deposited (a) Si/QHEA/Cu and (b) Si/SHEA/Cu film stacks (up-right corners: magnified images around HEA barrier layers).

film stacks seen in Fig. 3(a), the SEM surface and cross-sectional images of the 700 °C-annealed Si/QHEA/Cu film stack shown in Fig. 3(b) and (c) substantiated the severe interdiffusion and reactions along with the appearances of many compound phases and large pores. By contrast, for the Si/SHEA/Cu film stacks after annealing at 600–800 °C, the XRD patterns remained as the as-deposited feature. All the peaks sharpened with smaller full widths at half maximum (FWHM), and the intensities of either (1 1 1) or (2 0 0) peaks were enhanced owing to the grain growth of the Cu films from several tens to hundreds of nanometers as seen in the SEM images of the annealed samples shown in Fig. 3(d) and (e); in addition, no obvious agglomeration of the Cu films was found. Only two very small and indistinct diffraction peaks at about 45° appeared in the 800 °C-annealed Si/SHEA/Cu film stack, implying the beginning of interdiffusion at the high temperature; not any other obvious crystalline compound phases formed in the film stack after anneal-

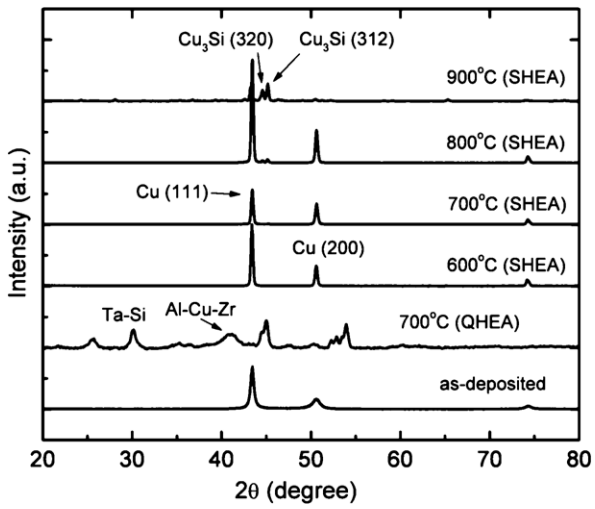

Fig. 2. XRD patterns of as-deposited and 600, 700, 800, and 900 °C-annealed Si/QHEA/Cu and Si/SHEA/Cu film stacks (Cu film thickness ~50 nm).

ing at 800 °C, suggesting the high endurance temperature of the ultra-thin SHEA barrier layer of only 5 nm thick. At an extremely high temperature of 900 °C, the SHEA barrier layer completely failed. A large number of Cu_3Si compound phase formed, as confirmed by the SEM image of the 900 °C-annealed Si/SHEA/Cu film stack shown in Fig. 3(f).

The variations in the sheet resistance of Si/QHEA/Cu and Si/SHEA/Cu film stacks after annealing, as plotted in Fig. 4, annotate the interdiffusion of Cu and Si through the QHEA and SHEA barrier layers. The resistance of as-deposited film stacks was determined as about 0.025–0.05 Ω/□. After annealing at 700 °C, due to the severe interdiffusion and reactions in the Si/QHEA/Cu film stack, the sheet resistance drastically increased to 6.6 Ω/□. In comparison, the resistance of the Si/SHEA/Cu film stack decreased to 0.021 Ω/□ at 700 °C and was further lowered to 0.014 Ω/□ at 800 °C owing to the grain growth and defect elimination of the Cu films, rather than any interdiffusion or film agglomeration. Only at 900 °C, the resistance of the Si/SHEA/Cu film stack jumped to 92.0 Ω/□, as a consequence of the failure of the SHEA barrier layer and the numerous formation of Cu_3Si compound phase.

Fig. 5 further shows the HRTEM images of the 700 °C-annealed Si/QHEA/Cu and 800 °C-annealed Si/SHEA/Cu film stacks. In Fig. 5(a), unclear interfaces between the Si substrate, native oxide layer, QHEA layer, and Cu film formed, implying the occurrence of

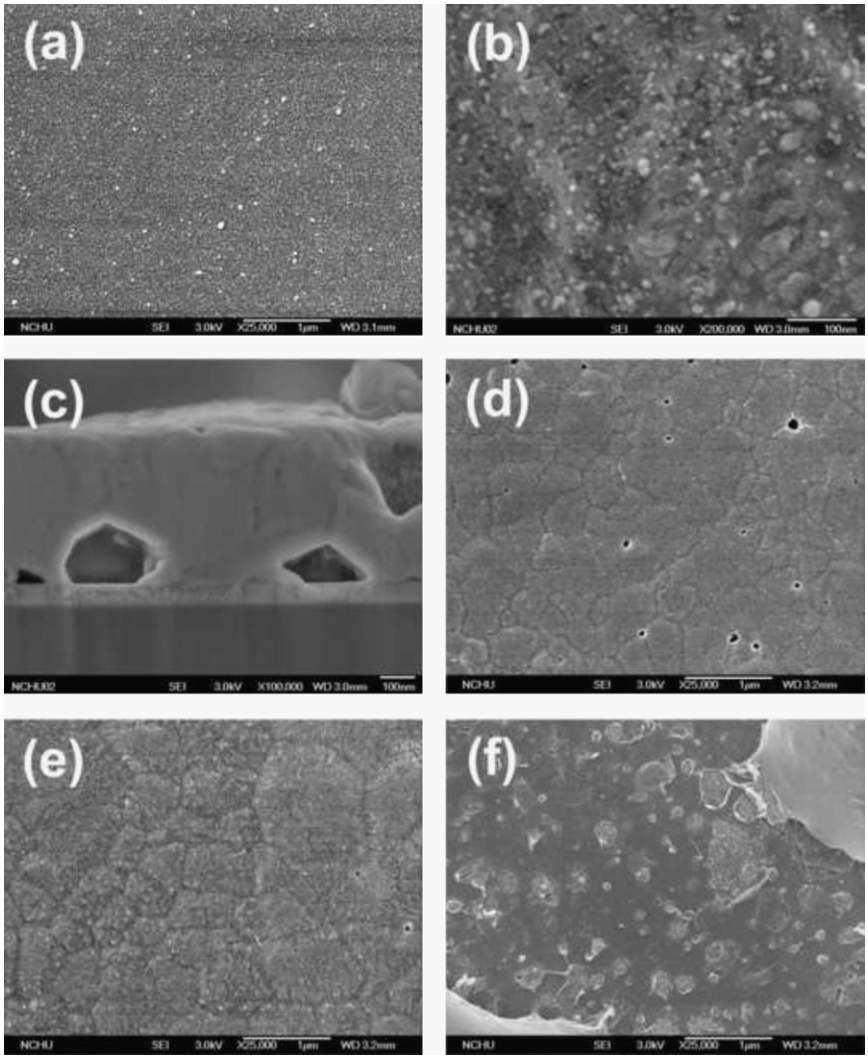

Fig. 3. (a) SEM surface morphology of typical as-deposited Si/HEA/Cu film stack; (b) surface morphology and (c) cross-sectional image of 700 °C-annealed Si/QHEA/Cu film stacks; surface morphologies of (d) 700 °C-, (e) 800 °C- and (f) 900 °C-annealed Si/SHEA/Cu film stacks.

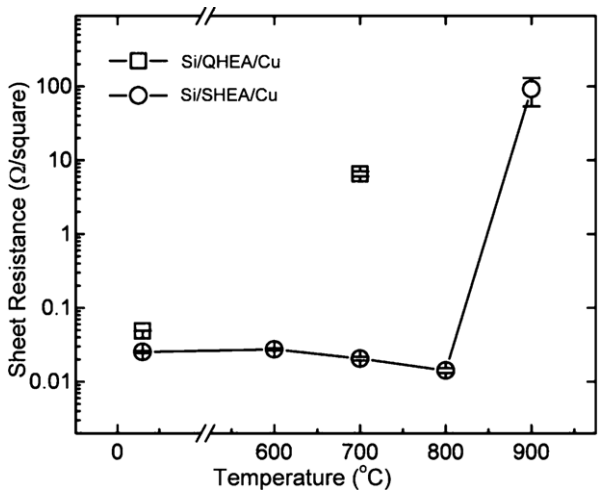

Fig. 4. Sheet resistance of as-deposited and 600, 700, 800, and 900 °C-annealed Si/QHEA/Cu and Si/SHEA/Cu film stacks.

interdiffusion and the failure of the QHEA barrier at 700 °C. As in the magnified image of the QHEA layer, the lattices of some silicides including Cu_3Si and Ta_5Si_3 were identified. In addition, the alloying of the metallic QHEA and penetrated Cu to construct $AlCu_2Zr$ as well as the crystallization of the amorphous QHEA to form Al_3Zr_4 were also observed. In comparison, at 800 °C, the interdiffusion of Cu and Si was still retarded by the SHEA layer as seen in Fig. 5(b); the Si/SHEA/Cu stacked structure and the lattice of Si substrate as well as the interfaces between each two layers were still clearly distinguished, along with the undamaged existence of the native oxide layer. However, because the SHEA layer was composed of only metallic elements rather than nitrides of strong covalent or ionic bonds, Cu penetration into the SHEA layer was anticipated. Thus as observed, some precipitates such as a Cu_9Al_4 formed around the SHEA/Cu interface. Crystallization of the amorphous SHEA layer into Al_3Zr_4 and Al_2Ti was also observed. Nevertheless, further Cu diffusion into the Si substrate was apparently retarded by the SHEA barrier layer; the ordered and perfect lattice structure of the Si substrate was still observed, suggesting the high diffusion resistance of the SHEA barrier layer consistent with above observations and analyses.

In comparison with some other reported benchmark barrier materials, e.g., TaN (30 nm thick [16]), Ru–Ti–N (10 nm [10]), Ru–Ta–N (15 nm [11]), TaN/Ta (10/20 nm [16]), and TaN/Ru (5/5 nm [17]), the metallic AlCrTaTiZrRu senary alloy film of 5 nm thick, despite the lack of strong ionic or covalent nitride bonds, exhibits an even superior performance and is highly promising for use as a diffusion barrier layer in advanced Cu interconnects. Two most important factors for the AlCrTaTiZrRu senary alloy functioning as an effective barrier layer are anticipated to be that the severely distorted lattices caused by the addition of multiprincipal elements with different atomic sizes (in particular by the incorporation of the extra-large atomic sized Ru) retard the diffusion of atoms and also that the amorphous film structure without grain boundaries reduces rapid diffusion paths, ultimately providing a high diffusion resistance. Especially for the former, relative to the average atomic size of the AlCrTaTiZr quinary alloy (2.84 Å, by the rule of mixtures), the extra-large size of Ru atoms (3.56 Å) generates a marked increase in the parameter *Delta*, which describes the comprehensive effect of atomic-size differences in multi-component alloys [27], from 8.26% to 11.85%. The hydrostatic compressive stresses around the Ru atoms or other elements with extra-large or much different atomic sizes are believed to reduce the molar volume of vacancies and consequently lower the diffusion coefficients of atoms in the AlCrTaTiZrRu senary alloy [28].

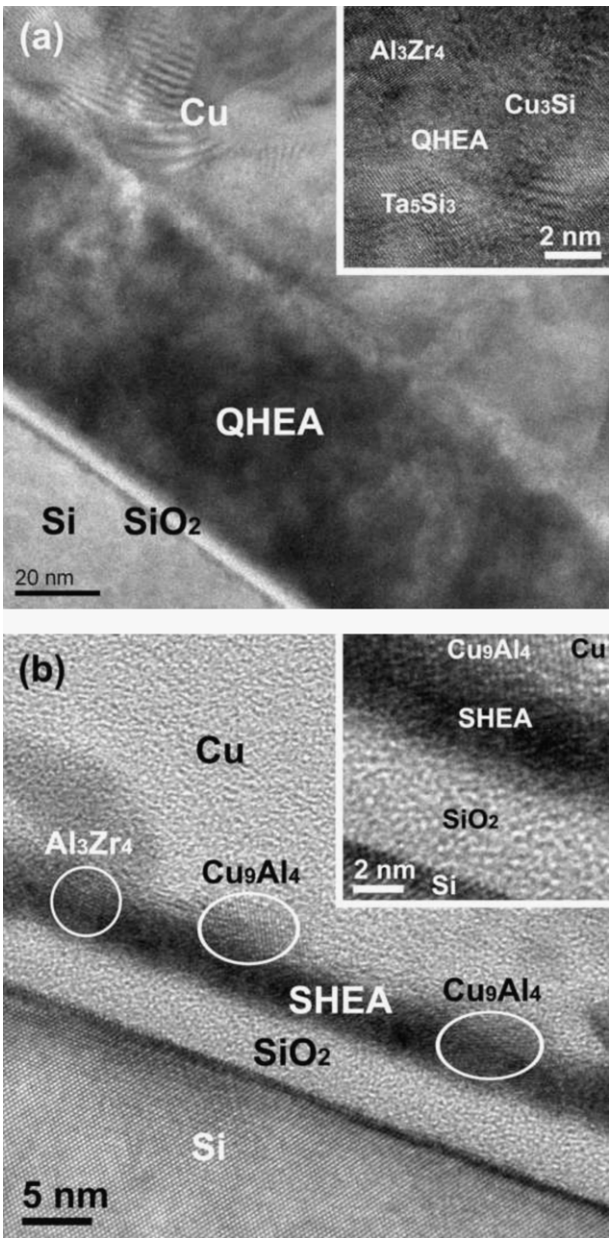

Fig. 5. HRTEM images of (a) 700 °C-annealed Si/QHEA/Cu and (b) 800 °C-annealed Si/SHEA/Cu film stacks (up-right corners: magnified images around HEA barrier layers).

4. Conclusions

In summary, amorphous AlCrTaTiZr quinary alloy and AlCrTaTiZrRu senary alloy films were developed in this study as diffusion barrier layers for Cu interconnects. From experimental results, it was known that the AlCrTaTiZr quinary alloy barrier layer of 50 nm thick failed at 700 °C. In comparison, the 20 at.% Ru-incorporated AlCrTaTiZrRu senary alloy layer of only 5 nm thick still presented a high resistance to the interdiffusion of Cu and Si at the temperature of 800 °C without obvious formation of silicides. Only at 900 °C, the AlCrTaTiZrRu barrier layer failed, and a large amount of Cu_3Si compound consequently formed. The high endurance temperature of the AlCrTaTiZrRu senary alloy was anticipated to be attributed to the large lattice distortions caused by the addition of extra-large-sized Ru atoms, besides the amorphous film structure.

Acknowledgements

The authors gratefully acknowledge the financial supports for this research by the National Science Council, Taiwan, under Grant No. NSC-98-2221-E-005-025, and in part by the Ministry of Education, Taiwan, under the ATU plan.

References

[1] E. Zschech, in: K. Wetzig, C.M. Schneider (Eds.), Metal Based Thin Films for Electronics, Wiley-VCH GmbH and Co. KGaA, Weinheim, Germany, 2003, p. 222.
[2] D.J. Kim, Y.T. Kim, J.W. Park, J. Appl. Phys. 82 (1997) 4847–4851.
[3] T. Kouno, H. Niwa, M. Yamada, J. Electrochem. Soc. 145 (1998) 2164–2167.
[4] K.H. Min, K.C. Chun, K.B. Kim, J. Vacuum Sci. Technol. B 14 (1996) 3263–3269.
[5] T. Oku, E. Kawakami, M. Uecubo, K. Takahiro, S. Yamaguchi, M. Murakami, Appl. Surf. Sci. 99 (1996) 265–272.
[6] Y. Liu, S. Song, D. Mao, H. Ling, M. Li, Microelectron. Eng. 75 (2004) 309–312.
[7] S.T. Lin, C. Lee, Appl. Surf. Sci. 253 (2006) 1215–1221.
[8] S. Rawal, D.P. Norton, H. Ajmera, T.J. Anderson, L. McElwee-White, Appl. Phys. Lett. 90 (2007) 051913.
[9] Y.L. Kuo, C. Lee, J.C. Lin, Y.W. Yen, W.H. Lee, Thin Solid Films 484 (2005) 265–271.
[10] S.H. Kwon, O.K. Kwon, J.S. Min, S.W. Kang, J. Electrochem. Soc. 153 (2006) G578–G581.
[11] C.W. Chen, J.S. Chen, J.S. Jeng, J. Electrochem. Soc. 155 (2008) H438–H442.
[12] P. Majumder, C.G. Takoudis, Appl. Phys. Lett. 91 (2007) 162108.
[13] Y. Wang, F. Cao, Y.T. Liu, M.H. Ding, Appl. Phys. Lett. 92 (2008) 032108.
[14] P. Majumder, C. Takoudis, Nanotechnology 19 (2008) 205202.
[15] L.C. Leu, D.P. Norton, L. McElwee-White, T.J. Anderson, Appl. Phys. Lett. 92 (2008) 111917.
[16] Q. Xie, X.P. Qu, J.J. Tan, Y.L. Jiang, M. Zhou, T. Chen, G.P. Ru, Appl. Surf. Sci. 253 (2006) 1666–1672.
[17] X.P. Qu, J.J. Tan, M. Zhou, T. Chen, Q. Xie, G.P. Ru, B.Z. Li, Appl. Phys. Lett. 88 (2006) 151912.
[18] Q. Xie, Y.L. Jiang, J. Musschoot, D. Deduytsche, C. Detavernier, R.L. Van Meirhaeghe, S. Van den Berghe, G.P. Ru, B.Z. Li, X.P. Qu, Thin Solid Films 517 (2009) 4689–4693.
[19] J.W. Yeh, S.K. Chen, S.J. Lin, J.Y. Gan, T.S. Chin, T.T. Shun, C.H. Tsau, S.Y. Chang, Adv. Eng. Mater. 6 (2004) 299–303.
[20] C.J. Tong, Y.L. Chen, S.K. Chen, J.W. Yeh, T.T. Shun, C.H. Tsau, S.J. Lin, S.Y. Chang, Metall. Mater. Trans. A 36A (2005) 881–893.
[21] C.J. Tong, M.R. Chen, S.K. Chen, J.W. Yeh, T.T. Shun, S.J. Lin, S.Y. Chang, Metall. Mater. Trans. A 36A (2005) 1263–1271.
[22] Y.Y. Chen, U.T. Hong, J.W. Yeh, H.C. Shih, Appl. Phys. Lett. 87 (2005) 261918.
[23] C.H. Lai, S.J. Lin, J.W. Yeh, S.Y. Chang, Surf. Coat. Technol. 201 (2006) 3275–3280.
[24] M.H. Tsai, C.W. Wang, C.H. Lai, J.W. Yeh, J.Y. Gan, Appl. Phys. Lett. 92 (2008) 052109.
[25] S.Y. Chang, M.K. Chen, D.S. Chen, J. Electrochem. Soc. 156 (2009) G37–G42.
[26] S.Y. Chang, D.S. Chen, Appl. Phys. Lett. 94 (2009) 231909.
[27] S.S. Fang, X.S. Xiao, L. Xia, W.H. Li, Y.D. Dong, J. Non-Cryst. Solids 321 (2003) 120–125.
[28] P.G. Shewmon, Diffusion in Solids, McGraw-Hill, New York, 1963, pp. 81–83.